Chapter III

Epoxidation and *cis*-dihydroxylation of olefins catalyzed by an oxo-bridged diiron(III) complex with H_2O_2

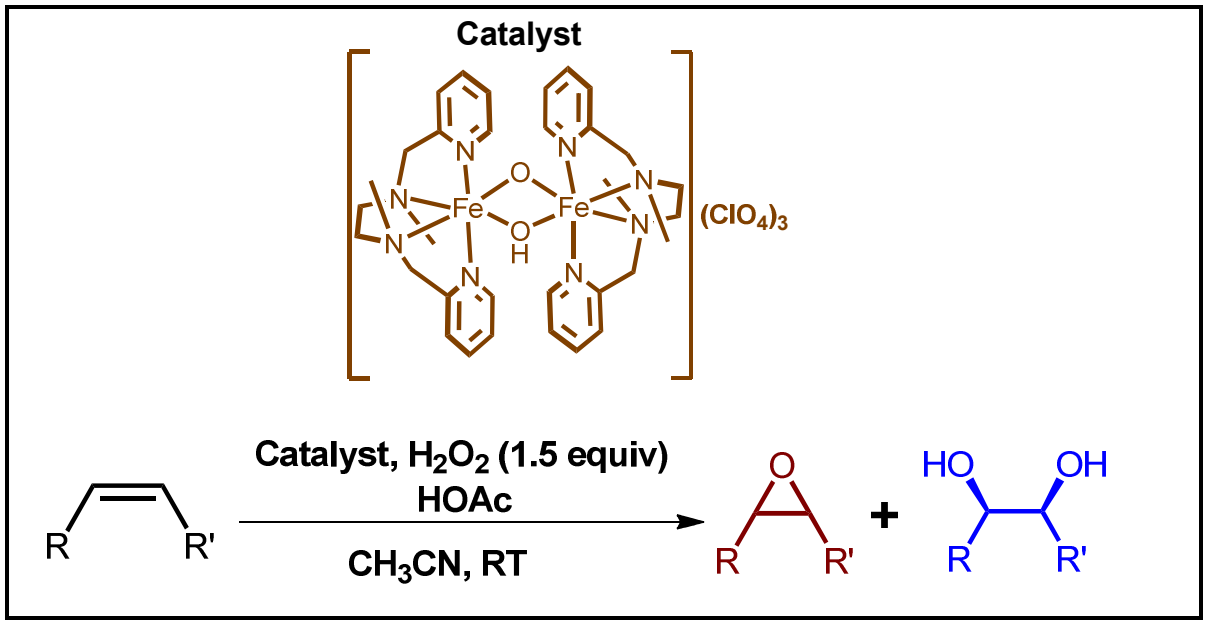

Chapter III

Abstract

Oxidation of olefins catalyzed by heme and non-heme enzymes with dioxygen or peroxides is known to yield epoxides. A notable exception is observed in the reactivity of the Rieske dioxygenases, wherein olefins get converted into *cis*-diols. Largely due to the seminal contribution from Professor L. Que, Jr. and co-workers, several bioinspired models for Rieske dioxygenases have been synthesized. Herein, the reactivity of a diiron(III) complex (**2**) based on tetradentate N4 ligand bpmen (bpmen = N,N´-dimethyl-N,N´-bis(2-pyridylmethyl)-ethane-1,2-diamine) with hydrogen peroxide under the conditions of limiting substrate is described. The symmetrical (μ-oxo)(μ-hydroxo)diiron(III) complex (**2**) is shown to be an excellent catalyst for oxidation of olefins at room temperature. The catalytic system has been shown to oxidize electron-deficient olefins to the corresponding *cis*-diols, while epoxidation is favoured in case of electron-rich olefins. The μ-oxo diiron(III) core of the catalyst **2** has been found be regenerated after the catalytic turnovers. Addition of second batch of substrate and oxidant at the end of the first cycle results in the formation of almost identical amounts of epoxides/diols. Interestingly, the regenerated catalyst exhibits a significantly higher preference towards the oxidation of electron-deficient olefins.

III.1. Introduction

Oxidative transformation of olefins into epoxides and *cis*-diols constitutes a key chemical process in synthetic organic chemistry [1-4]. Development of atom-efficient catalytic routes for olefin epoxidation/*cis*-dihydroxylation continues to be a major goal for synthetic chemists. Over the decades, considerable progress has been made in this area and several catalytic systems based on first-row transition metal complexes have been developed [5-12]. In particular, mononuclear non-heme iron(II) complexes based on tripodal pyridylamine ligands [13-15] (Scheme 1) have emerged as useful catalysts for the oxidation of olefins with mild hydrogen peroxide as the oxidant. These catalysts have been purposely developed to mimic iron enzymes such as Methane monooxygenase, Rieske dioxygenase *etc* [16].

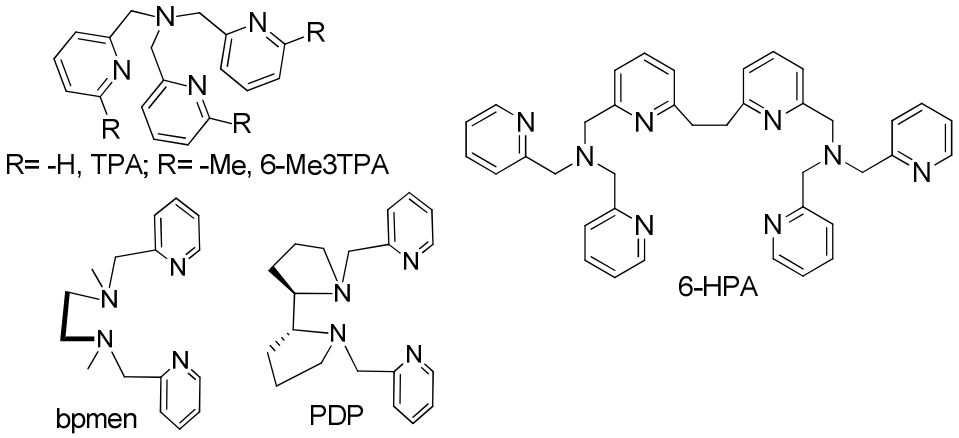

Scheme III.1 Polydentate ligands used in non-heme iron catalyzed alkene oxidation reactions.

Based on their pattern of reactivity, the iron(II)-catalysts have been categorized into two classes, viz., Class A & Class B catalysts [17]. Class A catalysts prefer electron-rich olefins and oxidize them into epoxides and cis-diols. In contrast, Class B catalysts preferentially react with electron-deficient olefins. Moreover, the diols derived in reactions catalyzed by the latter have been found to incorporate both the O-atoms from H_2O_2 [17]. So far, significant progress on the mechanistic details on the reactivity of the Class A catalysts has been made, wherein an electrophilic $Fe^{V}(O)(OH)$ species, generated from the heterolytic O-O bond cleavage of $Fe^{III}OOH$, has been implicated to be the active oxidant [18-21]. However, little is

known about the modus operandi of the Class B catalysts. Formation of a high-spin $Fe^{III}OOH$ species with a strong O-O bond has been suggested in this case. It is unclear whether the high-spin $Fe^{III}OOH$ species performs the *cis*-dihydroxylation directly or the putative oxoiron(V) intermediate formed *via* O-O lysis of $Fe^{III}OOH$ is the active oxidant.

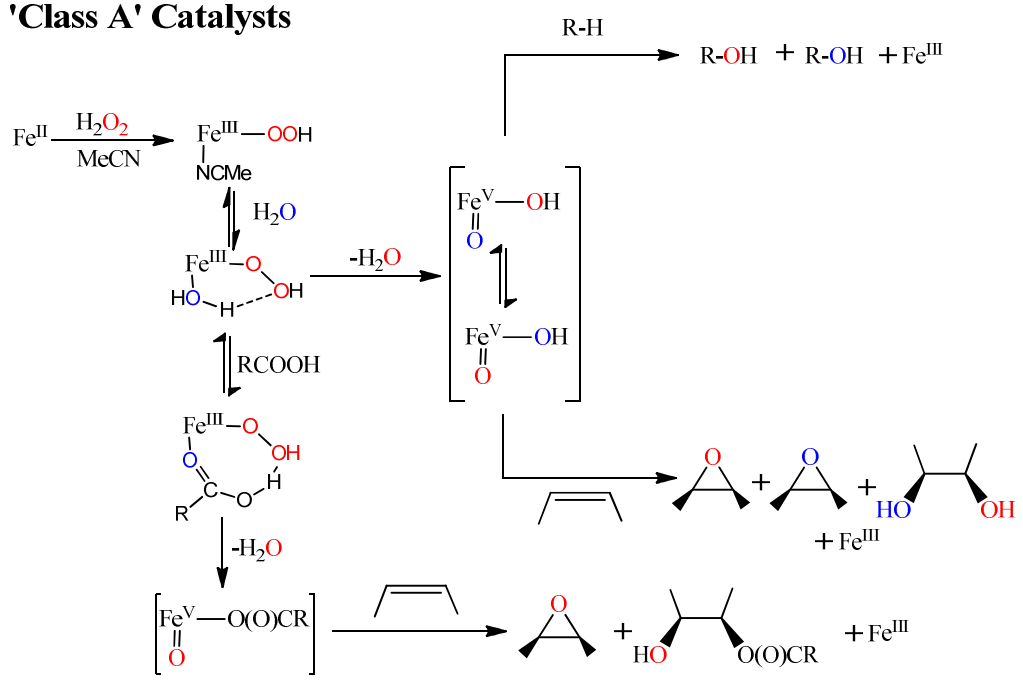

Scheme III.2 Proposed oxidation of alkanes and alkenes by nonheme Class A catalysts and hydrogen peroxide. Oxygen derived from H_2O_2 are shown in red, while oxygen atoms derived from water are shown in blue [19].

Several diiron catalytic systems have also been examined for olefin oxidation [22]. However, a vast majority of the oxo-bridged diiron complexes based on similar nitrogen rich ligands have exhibited rather sluggish oxidative reactivity [23-25]. Moreover, during the course of the catalytic reactions, the diiron catalysts have found to dissociate to monoiron complexes. For instance, cyclooctene oxidation by the mononuclear $[Fe^{II}(TPA)(MeCN)_2](ClO_4)_2$ and the corresponding diiron complex, $[Fe^{III}_2(O)(H_2O)_2(TPA)_2](ClO_4)_4$ have been shown to yield almost similar

amounts of epoxide and *cis*-diol, which, in turn, has been rationalized in terms of the dissociation of the diiron complex in solution [26]. In an effort to overcome this problem, Kodera and co-workers have recently developed a dinucleating ligand (6-HPA, Scheme 1) by introducing a -(CH_2CH_2)- spacer in between two tris-(2-pyridylmethyl)amine (TPA).

The (μ-oxo) diiron(III) complex of the dinucleating pyridyl ligand (6-HPA) was shown to be stable in solution and also during catalytic reactions with H_2O_2 [27]. In presence of excess cyclooctene and 150 equiv of H_2O_2 (*w.r.t.* the catalyst), the diferric catalytic system yields 105 turnovers of epoxide accounting for 70% of the oxidant.

Therefore, development of model systems with diiron core has to rely on the use of suitable ligand platform capable of stabilizing the dinuclear structure in solution. The catalytic results of the diiron complexes based on tripodal TPA ligand encouraged us to explore the catalytic potential of the oxobridged diiron(III) complex (**1**) of a linear aminopyridyl ligand, bpmen (Scheme III.1, bpmen = N,N´-dimethyl-N,N´-bis(2-pyridylmethyl)-ethane-1,2-diamine). The mononuclear iron(II) complex of the ligand, $[Fe^{II}(bpmen)]^{2+}$ (**1**) has previously been reported to be an excellent catalyst for epoxidation of olefins with H_2O_2 at room temperature [28]. The mononuclear complex **1** exhibits high reactivity towards electron-rich olefins and can be categorized as a Class A catalyst. Interestingly, ^1H NMR and EPR studies on the catalytic system **1**/H_2O_2 by Talsi *et al.* indicated the presence of the μ-oxo diiron(III) complex as the predominant species in acetonitrile solution [29]. At low temperature, the authors observed EPR signals characteristic of low-spin ferric hydroperoxo intermediates as well as a binuclear $Fe^{III}Fe^{IV}$ complex with localized antiferromagnetically coupled Fe^{III} (S=3/2) and Fe^{IV} (S=1) centres [29a]. The binuclear $Fe^{III}Fe^{IV}$ complex has been found to decay five times faster in presence of cyclohexene indicating that the species is involved in epoxidation of olefins by **1**/H_2O_2. Although epoxidizing ability of similar diiron species based on TPA ligand has already been established, the results disagree with the sluggish catalytic behaviour of μ-oxo diiron(III) complex based on bpmen ligand and H_2O_2 towards olefins [14,15].

Thus, the nature of the active species of **1**/H_2O_2 and **2**/H_2O_2 is far for being settled. Against this backdrop, we set out to explore the catalytic olefin oxidation by (μ-oxo)(μ-hydroxo)diiron(III) complex, [Fe_2(μ-O)(μ-OH)(bpmen)$_2$] (**2**) [30] with benign hydrogen peroxide as the terminal oxidant. The substrate-scope of **2**/H_2O_2 and the effect of acetic acid on olefin oxidation have been evaluated. Moreover, catalytic reactions have been performed under substrate limiting condition in order to demonstrate its suitability in preparative scale organic synthesis. In this contribution, we provide evidences to show that the reactivity of **2**/H_2O_2 towards olefins is markedly different from that of **1**/H_2O_2.

III.2. Results and discussion

III.2.1. Synthesis

The oxo-bridged diiron(III) complex was synthesized according to the literature procedure [31]. The reaction between bpmen [30] ligand and sodium hydroxide with iron(III) perchlorate salt in ethanol medium affords a deep maroon powder which was obtained after keeping the reaction mixture in refrigerator for overnight.

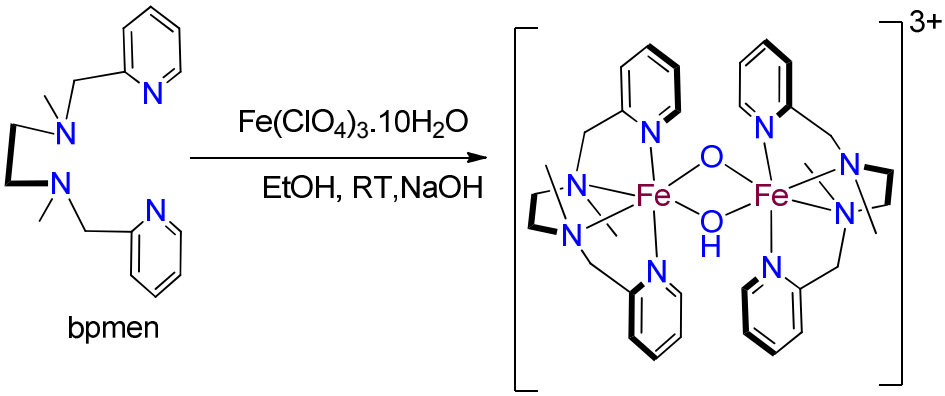

Scheme III.3 Synthesis of (μ-oxo)(μ-hydroxo) bridged diiron(III) complex containing bpmen ligand.

III.2.2. Characterization

III.2.2.1. Electronic spectra

The UV-visible spectra of complex **2** were recorded in acetonitrile. The corresponding spectra is shown in Fig III.1. The spectral data are given in Table III.1.

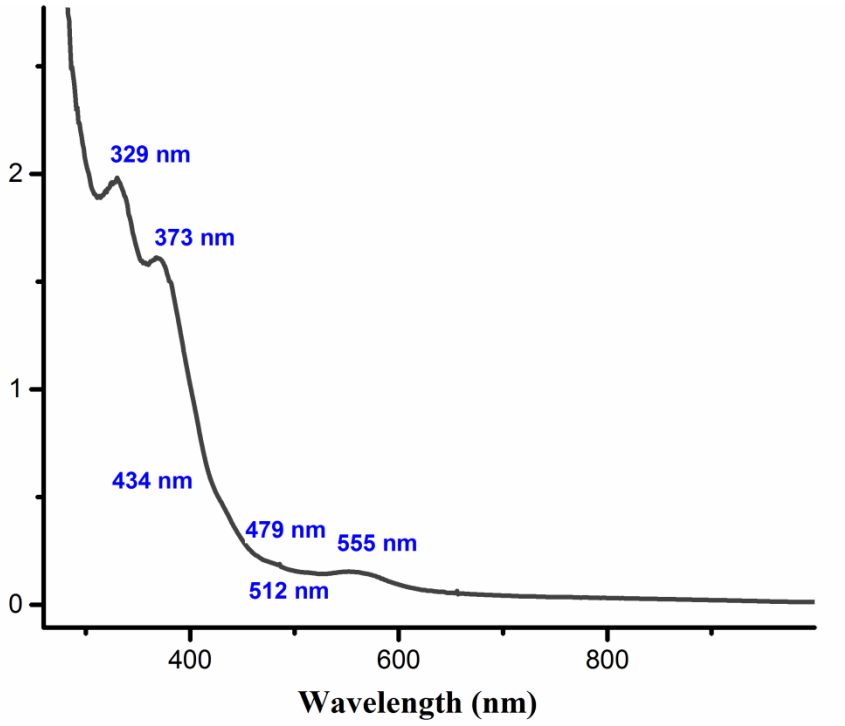

Fig III.1 UV-Vis spectra of the complex **2** in acetonitrile at room temperature (concentration of the complex = 2.5x 10^{-4} mM).

Table III.1 Electronic spectral data for **2** (2.5 X 10^{-4} mM) in acetonitrile.

	$\lambda_{max.}$ (nm)	ε (M^{-1} cm^{-1})
Complex **2**	329	6081
	373	4928
	434	1756(sh)
	479	670
	512	580
	555	693

It exhibit several peaks between the region 300-600 nm. The peaks around 373 are due to ligand-to-metal charge transfer transitions [32]. As with other µ-oxo –diiron(III) complexes, there is a band in the 400-550 nm region of medium intensity at 479 nm. This has been attributed to a $^6A_1 \rightarrow$ (^4E, $^4A_1$) transition, which is independent of the Fe-O-Fe angle [33]. The 550-700 nm region has been reported to be a signature of the Fe-O-Fe unit which strongly depends on the bridge angle [34]. Another significant feature of this core is a band at 555 nm. It is assignable to one of the bands usually observed in the 400-550 nm region of the electronic spectra of multiply bridged µ-oxo-diiron (III) complexes. As the Fe-O-Fe angle decreases the

intensity of the band increases. As previously mentioned by Hazell et al., [30a] the 555 nm band observed for this complex is associated with a significant red shift which is correlated with a closing of the Fe-O-Fe angle. As reported earlier [35] the 555 nm band would correspond to the angle of 111°. This really support the formation of the $[Fe(\mu\text{-}O)(\mu\text{-}OH)Fe]^{3+}$ core unit.

III.2.3. Catalytic properties

III.2.3.1. Oxidation of olefins by 2/H_2O_2

The oxo-bridged diiron(III) complex (**2**) has been found to be fairly stable in anhydrous acetonitrile at 25°C as no significant electronic spectral change of **2** is observed over 24 hours. The stability of the μ-oxo-diiron motif in 'neat' acetonitrile appeared promising and prompted us to explore the reactivity of the (μ-oxo) diiron(III) complex $[Fe_2(\mu\text{-}O)(\mu\text{-}OH)(bpmen)_2]$ (**2**) towards olefin oxidation with H_2O_2 at room temperature. To assess the potential of **2**/H_2O_2, *tert*-butyl acrylate, a prototype of electron-deficient alkenes, is chosen as the model substrate. So far, only a handful of catalytic systems have shown to be efficient in catalyzing *cis*-dihydroxylation of electron-poor olefins with H_2O_2 [13]. An efficient manganese based catalytic system for selective *cis*-dihydroxylation of electron deficient olefins with H_2O_2 has been reported by Saisaha *et al.* [36]. The manganese catalyst, prepared *in situ* by the reaction of a Mn(II) salt, pyridine-2-carboxaldehyde, a base and a ketone has exhibited high selectivity towards *cis*-dihydroxylation. An iron(III) catalyst based on a macrocyclic tetraza ligand has been shown to effective in catalyzing *cis*-dihydroxylation of electron poor olefins with oxone as the terminal oxidant[12]. Apart from these examples, a vast majority of catalysts based on inexpensive first-row transition metal complexes exhibit low to modest reactivity towards olefin *cis*-dihydroxylation [13].

Table III.2 Oxidation of *tert*-butyl acrylate by $[Fe_2(\mu\text{-}O)(\mu\text{-}OH)(bpmen)_2]$ (**2**) and H_2O_2 at room temperature:

Entry	Cat: Sub:HOAc:H_2O_2	Method[a]	Diol (%)[b]	Epoxide (%)[b]
1	1:20:0:30	A	17	06
2	1:20:1:30	A	25	04
3	1:20:0:30	B	28	08
4	1:20:1:30	B	60	0.3
5	1:40:1:60	B	55	0.1
6	1:60:1:90	B	45	0.2
7	1:100:1:150	B	17	02
8	3:100:3:150	C	64	0.2
9	1:20x(2):1:30x(2)	D	64	trace
10	1:20x(3):1:30x(3)	D	69	trace

[a]Method A: 37.5 mM (1.5 equiv. *w.r.t.* substrate) was added all at once;
Method B: 37.5 mM (1.5 equiv. *w.r.t.* substrate) was delivered by a syringe pump over 15 min at a rate of 0.6 mL/h;
Method C: Three iterative additions of **2** (3 mol%), AcOH (3 mol%) and H_2O_2 (0.5 equiv. *w.r.t.* substrate).
Method D: Additional aliquots of H_2O_2 (37.5 mM, 1.5 equiv. *w.r.t.* substrate) and substrates were delivered at the end of the reactions.
[b]Yields are based on the substrate concentration. See Experimental Section for details.

The results encouraged us to explore the catalytic reactivity of the diiron(III) catalyst (**2**) towards electron-poor olefins. The catalytic reactions have been performed in acetonitrile medium by both syringe-pump as well as all-at-once addition of H_2O_2 (Table III.3). As shown in Table III.2, using catalyst **2 (**5 mol%), oxidation of *tert*-butyl acrylate affords the 17% *syn*-diol and 6% epoxide in acetonitile at room temperature (298 K) (Entry 1, Table III.2). When the reaction is carried out in presence of one-equivalent acetic acid (*w.r.t.* **2**), modest improvement of substrate conversion is observed (Entry 2, Table III.2). In order to further improve the catalyst turnovers and substrate conversion, H_2O_2 (1.5 equiv. *w.r.t.* the substrate) has been delivered over a

period of 15 min at a rate of 0.6 mL/h. Under the syringe pump addition protocol, significant improvement substrate conversion (Entry 4, Table III.2) is observed and the corresponding *syn*-diol is obtained as the major product. However, increasing the amount of substrate under identical reaction condition has been found to result in poor substrate conversion. As shown in Table III.2, employing a catalyst:substrate:HOAc: H_2O_2 of 1:100:1:150, only 17% *syn*-diol and 2% epoxide are obtained indicating significant catalyst deactivation. In order to overcome it, three iterative additions of the catalyst **2,** HOAc and the oxidant H_2O_2 has been designed. Under iterative addition protocol, yield of the diol increases up to 64% (Entry 7 & 8, Table III.2). It is noteworthy in this regard that oxidation of *tert*-butyl acrylate catalyzed by the monomeric iron(II) complex of bpmen [(bpmen)$Fe^{II}(OTf)_2$] [19,28,37] and H_2O_2 has been shown to afford both epoxide and diol with a slight preference for the diol product over epoxide (epoxide/diol = 1:1.5). Furthermore, addition of acetic acid dramatically improved epoxide selectivity (epoxide/diol = 5:1). Therefore, in order to have further insight into the catalytic reactivity of complex **2**, attempts have also been made to assess the amount of catalytically reactive species at the end of the reaction. Thus, after delivering H_2O_2 (75.0 μmol, 1.5 equiv. *w.r.t.* the substrate) in acetonitrile medium containing 5 mol% (2.5 μmol) of **2** and HOAc, followed by stirring the reaction mixture for an additional 15 min, a second aliquot of both the substrate and oxidant have been added in an identical fashion. Interestingly, the catalytic system has been found to exhibit almost identical reactivity (Entry 9, Table III.2). The reactivity remains unchanged even after the third addition of substrate and oxidant indicating almost complete regeneration of the oxidizing species at the end of each catalytic cycle.

The substrate scope of the present catalytic system has also been examined and the results are summarized in Table III.3. In all catalytic reactions, the ratio of catalyst:substrate:HOAc:H_2O_2 of (1:20:1:30) has been maintained and the oxidant is delivered over a period of 15 min (*vide* Experimental Section for details). For the electron deficient olefins, *cis*-diols are obtained as the major product with modest yields. Oxidation of dimethyl fumarate afforded the *cis*-diol product, *d/l*-dimethyl

tartarate as the major product with high diol selectivities, *viz.*, diol/epoxide ratio of 7.5 which shoots up to 22 in presence of 2.5 µmol acetic acid in acetonitrile at room temperature (Entries 1 & 2, Table III.3). Oxidation of ethyl crotonate yielded a mixture of *cis*-diol and epoxides with higher selectivity for the diol (D/E of 4.0, Entry 5, Table III.3). In presence of acetic acid, a clear preference for the formation of *cis*-diol product, as evident from a D/E value of 14.3, is observed (Entry 6, Table III.3). Oxidation of other electron-deficient olefins, *viz.*, acrylonitrile, diethyl maleate and 2-cyclohexene-1-one also exhibited similar product profile under identical reaction condition (Table III.3). Oxidation of methyl cinnamate under similar reaction condition results in the formation of diols and epoxide with somewhat lower yields (Entry 7 & 8, Table III.3). In this case, preliminary studies have indicated a competitive oxidation of the phenyl ring of the substrate by **2**/H_2O_2(AcOH), which, in turn, rationalizes the lower yield of the products derived from the C=C oxidation. The reactivity of the present catalytic system towards arene hydroxylation has been discussed in chapter IV. Oxidation of electron-rich olefins by **2**/H_2O_2 exhibits a complete reversal in product profile with epoxides as the major products with minor amounts of *cis*-diols. The electron-rich *cis*-cyclooctene has been converted to the cyclooctane oxide in 60% yield. A small amount of the corresponding *cis*-diol product (10%) has also been obtained (Entry 13, Table III.3). Addition of **1** equiv. of acetic acid prior to the addition of the substrate results in considerable increase in the product yield (87%) based on the initial substrate concentration (Entry 14, Table III.3). In case of oxidation of 1-octene by **2**/H_2O_2, overall yield of oxygenates reaches 50% with an epoxide/*cis*-diol ratio of 4.0. Moreover, combined yields of epoxide and *cis*-diol as well as the epoxide selectivity have been found to increase in presence of one equivalent of AcOH (Entries 15 & 16, Table III.3).

Table III.3 Oxidation of olefins by $[Fe_2(\mu\text{-}O)(\mu\text{-}OH)(bpmen)_2]$ (**2**) and H_2O_2 in acetonitrile at room temperature[a].

Entry	Substrate	HOAc (equiv.)	Yield[b] (%)	Diol[b] (%)	Epoxide[b] (%)	D/E
1	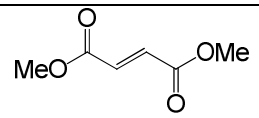	-	34	30	04	7.5
2		1.0	46	44	02	22
3	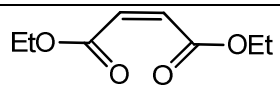	-	12	10	2	5
4		1.0	36	33	3	11
5	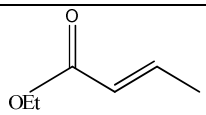	-	25	20	5	4
6		1.0	46	43	3	14.33
7	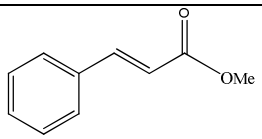	-	12	9	3	3
8		1.0	26	21	5	4.2
9	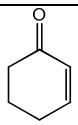	-	9	6	3	2
10		1.0	20	14	4	3.5
11	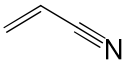	-	19	16	03	5.33
12		1.0	40	39	01	39
13		-	70	10	60	0.167
14		1.0	87	03	84	0.036
15	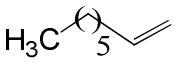	-	50	10	40	0.25
16		1.0	66	04	62	0.065
17	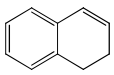	-	30	10	20	0.5
18		1.0	38	08	30	0.267
19	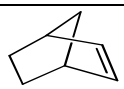	-	38	12	26	0.46
20		1.0	38	08	30	0.267
21		-	75	-	50 (*cis*) 25(*trans*)	-
22		1.0	78	-	70 (*cis*) 08(*trans*)	-

[a]H_2O_2 was delivered by syringe pump over 15 min at a rate of 0.6 mL/h and 15 extra minutes of stirring were allowed before workup. [b]Yields are based on substrate concentration.

Olefin epoxidation catalyzed by **2**/H_2O_2 has exhibited a modest degree of retention of configuration in case of *cis*-stilbene, a 1,2-disubstituted alkene. Oxidation of *cis*-stilbene under identical reaction condition yielded the corresponding epoxide with 50% retention of configuration. However, in presence of one equivalent AcOH, the epoxide product was formed with more than 80% retention of configuration (Table III.3). Such a high degree of stereo-retention further supports the involvement of a metal-based oxidant in the present oxidizing system [38].

In order to evaluate the nature of oxidant in the present catalytic system, competitive olefin oxidation reactions under similar reaction condition were performed. Equimolar amounts of a pair of olefin substrates have been oxidized by **2**/H_2O_2 either in presence or in absence of AcOH. The results are presented in Fig III.2 and Table III.4.

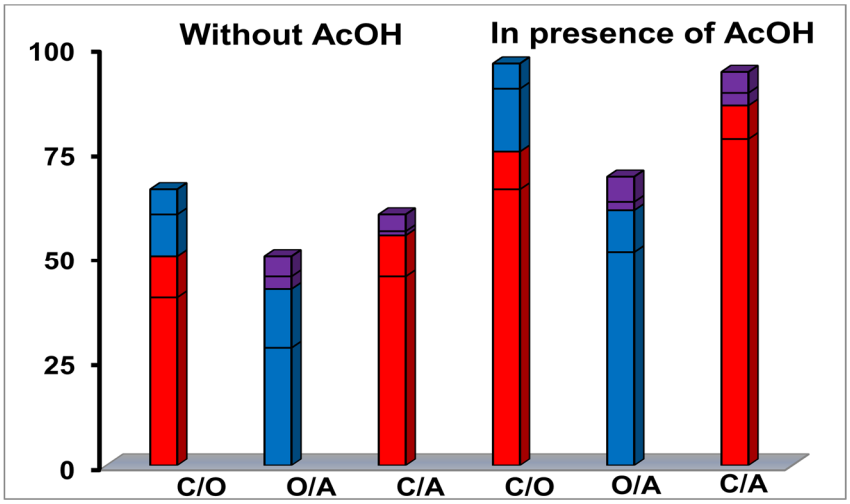

Fig III.2 Competitive experiments for the oxidation of different olefin pairs by **1**/H_2O_2. C= cyclooctene (red), O = 1-octene (blue), A = *tert*-butyl acrylate (purple). Lower blocks represent the amount of epoxide formed while the upper blocks represent the amount of *cis*-diol formed.

Table III.4. Competitive oxidation of olefins catalyzed by [Fe_2(μ-O)(μ-OH)(bpmen)$_2$] (**2**) and H_2O_2 at room temperature.

Entry	Substrates[a]	Product yield (%)[b]			
		Olefin A[c,d]		Olefin B[c,d]	
		Epoxide	Diol	Epoxide	Diol
1	*Cis*-cyclooctene & 1-octene	40 [66]	10 [09]	10 [15]	06 [06]
2	1-octene & *tert*-butyl acrylate	28 [51]	14 [10]	03 [02]	05 [06]
3.	*Cis*-cyclooctene & *tert*-butyl acrylate	45 [78]	10 [08]	01 [03]	03 [05]

[a]Equimolar ratio (1:1) of two substrates; [b]Yields are based on initial concentration of the substrate; [c]For a pair of olefin, 'olefin A' refers to the more electron rich substrate while 'olefin B' refers to the less electron rich substrate; [d] Products yields in presence of 1.0 equiv. of acetic acid are given in the parenthesis.

The competitive oxidation of *cis*-cyclooctene and *tert*-butyl acrylate, cyclooctene oxidation yields 55% products (epoxide/diol = 4.5:1) while only 4% oxygenates (epoxide/diol = 1:3) are obtained from *tert*-butyl acrylate oxidation. Moreover, in presence of AcOH, catalyst **2** favoured the oxidation of electron-rich cyclooctene by a factor of 10.75 (Figure III.2). The results are indicative of the formation of an electrophilic oxidant in the present oxidizing system [18, 19].

During the course of the evaluation of the catalytic efficacy of **2**/H_2O_2, compelling evidences indicated that the initial catalyst **2** and the regenerated catalyst (**2′**) at the end of the reaction exhibit different reactivity patterns. In order to showcase the reactivity difference, **2′** was generated *in situ* by the reaction of **2** (2.5 μmol) and H_2O_2 (75 μmol) in acetonitrile and an equimolar mixture of *cis*-cyclooctene and *tert*-butyl acrylate (50 μmol each) is introduced as substrates. Unlike catalyst **2**, the regenerated catalyst has exhibited a significant preference towards the oxidation of electron-poor acrylate. Product analysis reveals the formation of 87% oxygenates from

cyclooctene oxidation (epoxide/diol= 28) and 44% oxygenates from acrylate oxidation [39]. The regenerated catalyst favours oxidation of *cis*-cyclooctene over acrylate by a factor of only 2.0 (Table III.5)

Table III.5 Competitive oxidation of olefins catalyzed by the regenerated catalyst (**2**') and H_2O_2 at room temperature

Substrates[a]	Product yield (%)[b]			
	Cyclooctene		Tert-butyl acrylate	
	Epoxide	Diol	Epoxide	Diol
Cis-cyclooctene & *tert*-butyl acrylate	84%[b]	03%[b]	02%[b]	42%[b]

[a]Equimolar ratio (1:1) of two substrates; [b]The yields are based on the initial substrate concentrations.

Comparing the results (Table III.5) with those obtained with **2**/H_2O_2 (Table III.4), significantly higher preference of **2′** towards the oxidation of electron deficient olefins is observed. The results clearly point out that the key oxidizing species responsible for olefin oxidation is less electrophilic in nature compared to that involved in the parent catalyst.

Moreover, the catalytic efiicacy of the present catalytic system was explored by using a large excess of the olefin (1000 equiv./catalyst) and 100 equiv./catalyst of oxidant. Under the reaction condition cyclooctene has been found to be converted into a mixture of epoxide and *cis*-diol in 40% and 5% yields respectively. Furthermore, the catalytic efficacy of complex **2** increased considerably upon addition of 1 equiv. acetic acid prior to the addition of H_2O_2 (Table III.6). In presence of acid turnover number (TON) based on complex **2** reached 65 and only a trace amount (2%) of *cis*-diol was obtained. As shown in Table III.6, epoxidizing ability of **2**/H_2O_2/AcOH is comparable to that obtained with the (μ-oxo) diiron(III) complex of a dinucleating pyridyl ligand (6-HPA) reported recently by Kodera *et al*.. In this case, 70% of the oxidant has been accounted for the products. In comparison, 65% of the total H_2O_2 has been shown to be converted into mainly epoxides during oxidation of *cis*-cyclooctene by the present catalytic system (**2**/H_2O_2).

Table III.6 Oxidation of cyclooctene catalyzed by non-heme iron catalysts with H_2O_2 as the oxidant.

Catalyst	Equiv. H_2O_2[a]	Equiv. AcOH	Yield (%)[b]	Products (TON)[c]	Ref
[(6-HPA)Fe^{III}_2O]	150	-	70	Epoxide (105) *Cis*-diol (03)	27a
[Fe_2(μ-O)(μ-OH)(bpmen)$_2$] (**2**)	100	-	45	Epoxide (40) *Cis*-diol (05)	This work
	100	1.0	65	Epoxide (63) *Cis*-diol (02)	This work
$[Fe^{II}(bpmen)]^{2+}$	300	12000	90	Epoxide (187)	19
$[Fe^{II}(TPA)]^{2+}$	300	12000	90	Epoxide (185)	19

[a]Equivalent of H_2O_2 *w.r.t.* the catalyst; [b]Based on initial concentration of the oxidant; [c]TON = amount of products/amount of the catalyst

III.2.3.2. Mechanistic Aspects

So far, a number of nonheme iron(II) complexes have been shown to catalyze epoxidation and *cis*-dihydroxylation of olefins with H_2O_2 as the terminal oxidant [3, 13, 17-19] Depending on the nature of ligands, several high-valent oxo-iron intermediates have been suggested as the key intermediate. In particular, a putative oxoiron(V) intermediate, *cis*-HO-Fe^{V}=O has been invoked as the active oxidant in *cis*-hydroxylation of olefins [40, 41]. Indeed, such species has recently been detected by variable temperature mass spectrometry [42].

In contrast, a $Fe^{III}(\eta^2$-OOH) has been suggested as the active oxidant in case of olefin *cis*-dihydroxylation catalyzed by Rieske dioxygenases [43]. Very recently, Talsi and co-workers have provided convincing EPR evidence supporting the formation of a formal oxoiron(V) species from dinuclear iron(III) complexes (bearing aminopyridine ligands TPA*/or PDP*, [TPA*=tris(3,5-dimethyl-4-methoxypyridyl-2-methyl)amine, PDP* = bis(3,5-dimethyl-4-methoxypyridyl-2-methyl)-(S,S)-2,2'-bipyrrolidine] with H_2O_2 and acetic acid [44]. In presence of acetic acid, the dinuclear iron(III) complexes were shown to get converted into monomeric ferric complexes of the type $[(L)Fe^{III}(\kappa^2$-$(OC(O)CH_3]^{2+}$, which, reacts with H_2O_2 to generate formally oxoiron(V) intermediate [either(L)Fe^{V}=O or $(L^{\bullet+})Fe^{IV}$=O].

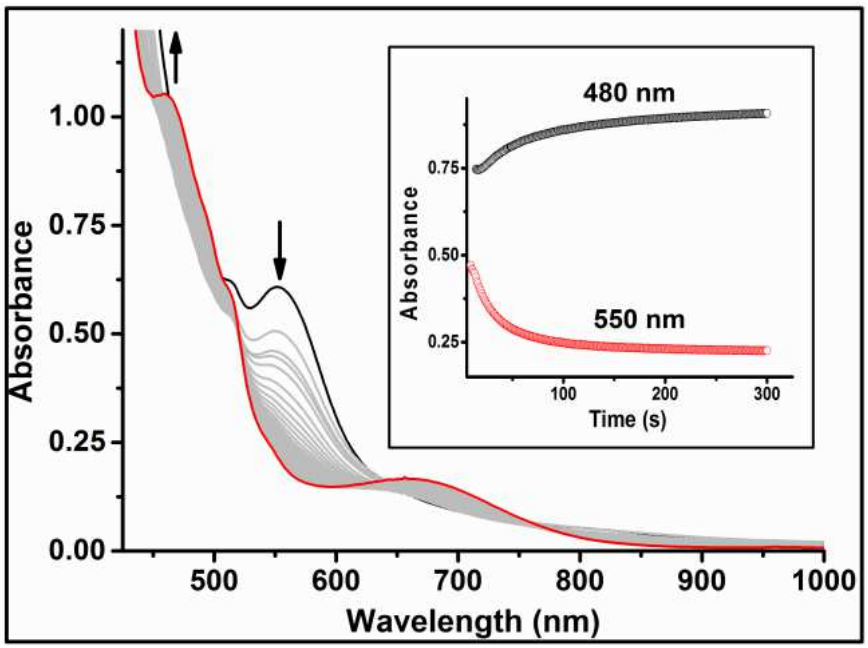

Fig III.3 UV-vis spectral changes obtained upon the addition of H_2O_2 (30 mM) to a solution of complex **2** (1 mM) and *tert*-butyl acrylate (20 mM) in neat acetonitrile at 298 K. Inset: Change of absorbance of the 480 and 550 nm bands monitored with time.

The putative species is claimed to be the active oxidant in olefin oxidation. Given the structural similarity of bpmen ligand with PDP*, formation of putative oxoiron(V) species in the present case cannot be overruled. This prompted us to examine the fate of the oxo-bridged diiron(III) complex (**2**) at the end of the catalytic reactions. Thus, the oxidation of *tert*-butyl acrylate by **2**/H_2O_2 in acetonitrile at 298 K is monitored by UV-vis spectroscopy. Electronic spectrum of complex **2** in neat acetonitrile exhibits a weak absorption at 550 nm, which is a signature of the Fe(III)–(μ-O)–Fe(III) core originating from $^6A_1 \rightarrow (^4A_1, {}^4E)$ transition. Upon addition of excess H_2O_2 to complex **2**, the intensity of the 550 nm absorption decreases rapidly followed by the appearance of new absorption features around 350, 430 and 512 nm (Figure III.3). The final electronic spectrum is then compared with that of the starting complex (**2**) (Figure III.4). The spectrum of the regenerated catalyst resembles that of $[(bpmen)(H_2O)Fe(\mu\text{-}O)Fe(OH)(bpmen)]^{3+}$, [45] previously observed by Poussereau *et al.* upon addition of water to an acetonitrile solution of complex **2**.

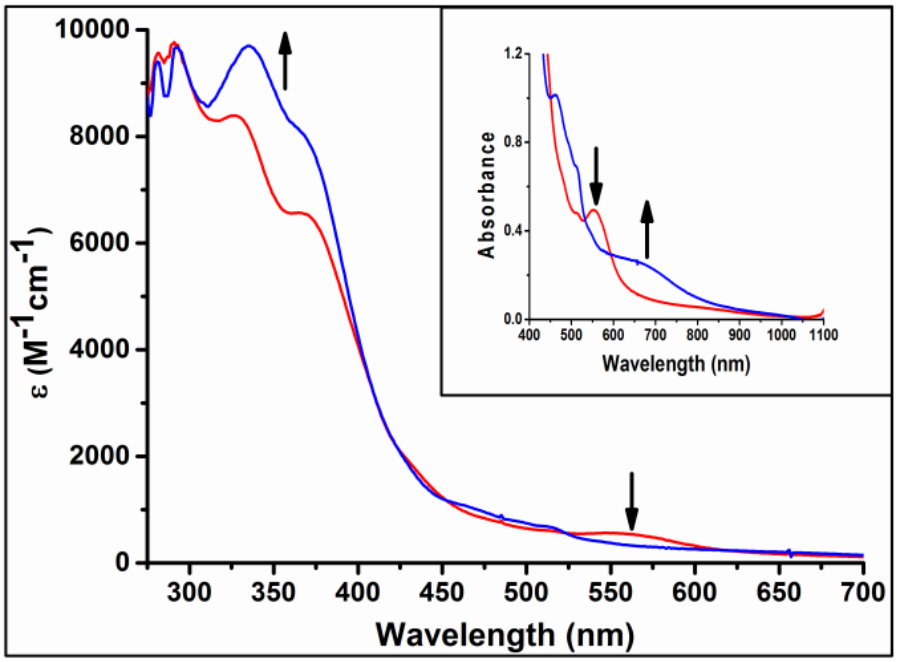

Fig III.4 UV-vis spectrum of the complex **2** (1.25 x 10^{-4} M) (red line) and that of the species obtained at the end of the aromatic hydroxylation (blue line) in dry acetonitrile at 298K. The final spectrum corresponds to the complex $[(bpmen)(H_2O)Fe(\mu\text{-}O)Fe(OH)(bpmen)]^{3+}$ (**2'**) Inset: Electronic spectra of **2** and **2'** in the visible region in dry acetonitrile at 298 K.

The rate of formation of the open core oxo-bridged diiron(III) complex has been found to increase in presence of AcOH (Fig III.5).

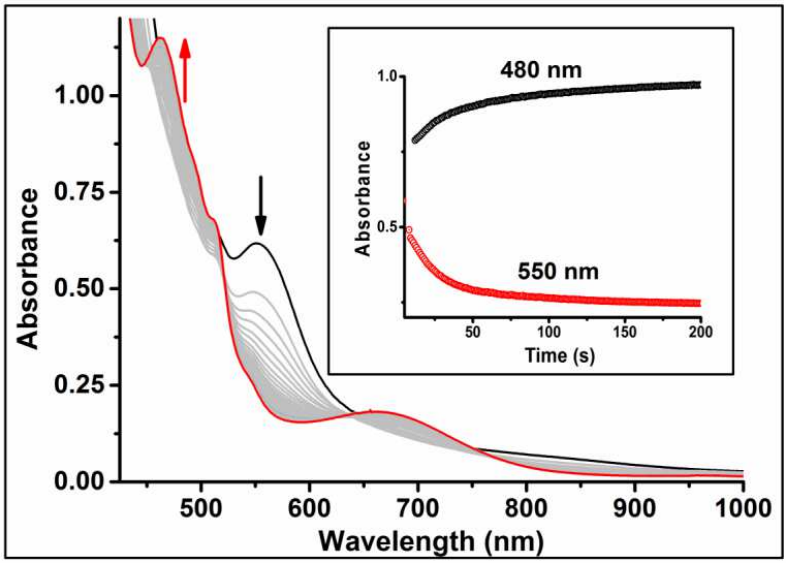

Fig III.5 UV-vis spectral changes obtained upon the addition of H_2O_2 (30 mM) to a solution of complex **2** (1 mM), AcOH (1 mM) and *tert*-butyl acrylate (20 mM) in neat acetonitrile at 298 K. Inset: Change of absorbance of the 480 and 550 nm bands monitored with time.

The electronic spectral changes can be rationalized in terms of rapid rupture of μ-oxo diiron core to generate a monoiron species, which ultimately converts to the thermodynamically more stable Fe(III)–(μ-O)–Fe(III) complex. Additional evidences in favour of this hypothesis have been obtained from EPR studies. The starting diiron(III) complex (**2**) is EPR silent. However, after the addition of 10 equiv. of H_2O_2 to an acetonitrile solution of complex **2** (1 mM) at room temperature and freezing the mixture at -78°C, the EPR spectrum (Fig III.6) exhibits a signal at g = 4.23, which can be tentatively assigned to a high-spin mononuclear iron(III) complex. Moreover, the spectrum also indicates the presence of at least two S=1/2 species in the mixture (Fig III.6).

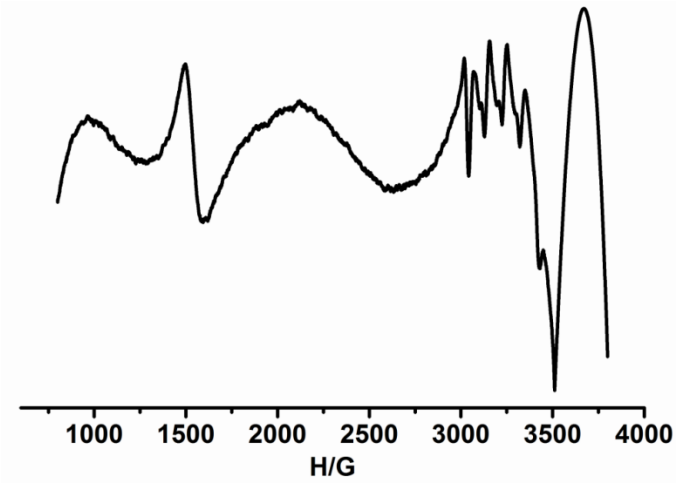

Fig III.6 X-band EPR spectrum obtained after the addition of 10 mM H_2O_2 to an acetonitrile solution of **2** (1.0 mM) at 298 K followed by rapid freezing of the solution.

The resonances at g_1 = 2.15, g_2 = 2.15 and g_3 = 2.08 can be rationalized either by considering the formation of a low-spin ferric hydroperoxo intermediate or a binuclear $Fe^{IV}Fe^{III}$ complex with antiferromagnetically coupled Fe^{III} (S = 3/2) and a low-spin Fe^{IV} (S=1) unit [29]. At this point, unambiguous assignment of the EPR signals could not be made due to rather low concentration of this species (<5% of the total iron concentration in the sample). The second set of signals appears at g_1 = 2.06, g_2 = 2.01 and g_3 = 1.96. It is noteworthy that an S=1/2 EPR signal similar to the latter has recently been detected by Talsi *et al.* in reactions between structurally related oxo-bridged diiron(III) complex and H_2O_2 at low temperature [44]. The authors assigned this signal to a highly reactive formally oxoiron(V) intermediate.

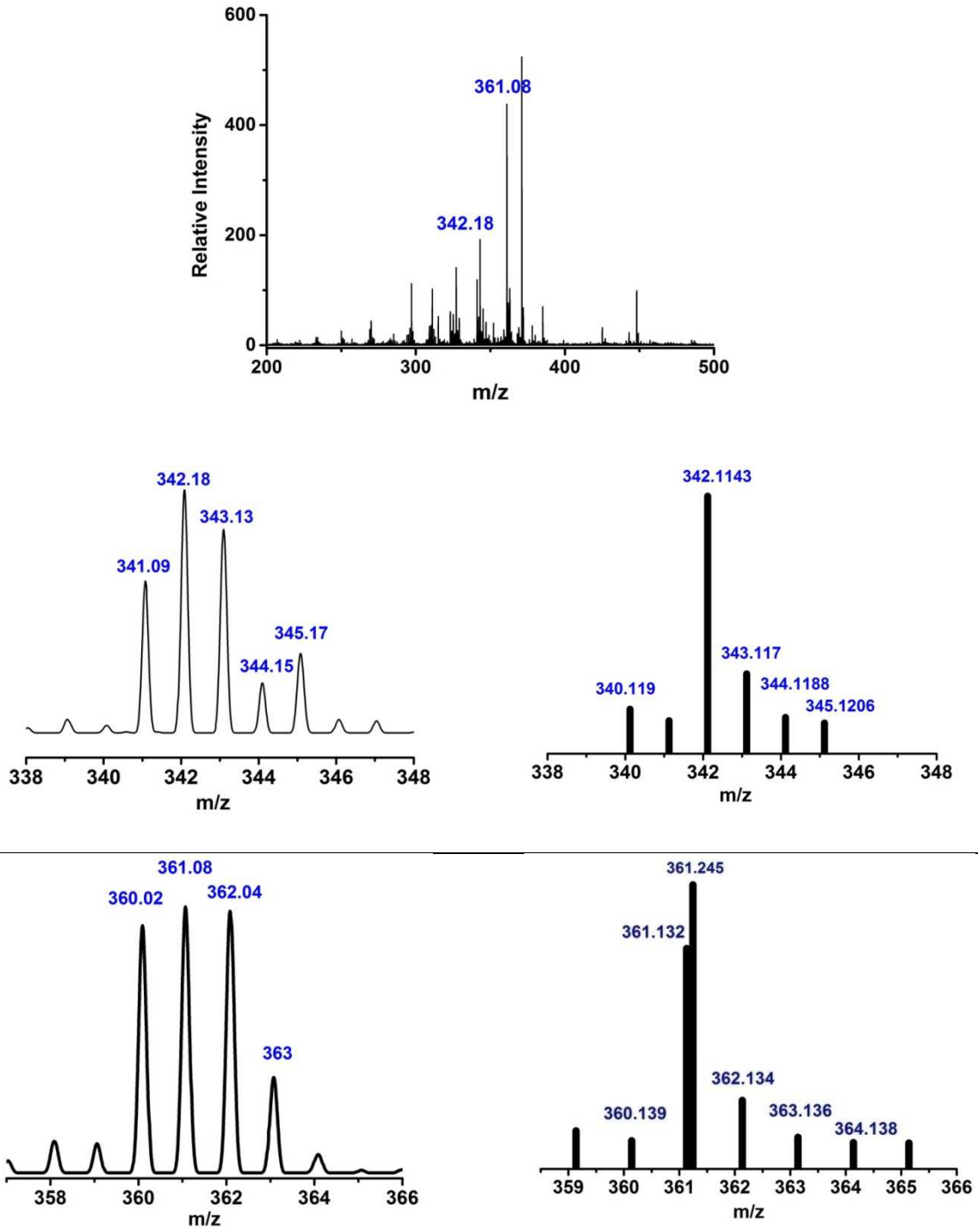

Fig III.7 ESI-MS spectrum obtained immediately after the addition of 10 mM H_2O_2 to an acetonitrile solution of **2** (1.0 mM) at 298 K (Above). The experimental and theoretical isotope distribution patterns for the peaks at m/z 342 and 361 (Below). The peak at m/z = 342 has been assigned to $[(bpmen)Fe^{III}(O)]^+$ whereas the peak at m/z = 361 can be assigned to the species $[\{(bpmen)Fe^{III}(O)(OH_2)\}+H]^+$.

Therefore, it is reasonable to believe that in the present case, a putative oxoiron(V) species may serve as one of the active intermediates. Formation of appreciable amounts of *cis*-diols in alkene oxidation catalyzed by **1**/H_2O_2 is also in agreement with this hypothesis. Both the sets of resonances have been found to decay with time and ultimately yield an EPR silent species, presumably the open core Fe(III)–(μ-O)–Fe(III) species (**2'**). Formation of the monoiron species during catalysis has also been supported by the *in situ* ESI-MS analysis. ESI-MS spectrum obtained after the addition of H_2O_2 to an acetonitrile solution of **2** (Fig III.7) exhibits prominent peaks at *m/z*=342 and 361, which can be tentatively assigned to the $[(bpmen)Fe^{III}(O)]^+$ and $[\{(bpmen)Fe^{III}(O)(OH_2)\}+H]^+$.

We have also scrutinized whether the catalytic reactivity of complex **2** is due to the *in situ* generated (μ-oxo)(μ-acetato)diiron(III) complex as previously reported by Jacobsen *et. al*. [28]. Independently synthesized (μ-oxo)(μ-acetato)diiron(III) (**3**) has been found to be inefficient in catalyzing olefins under similar reaction condition as only traces of epoxide from *cis*-cyclooctene have been obtained. Even in presence of excess acetic acid, **3**/H_2O_2 exhibits poor oxidative reactivity towards olefins. The present results corroborates with the previous results, wherein the (μ-oxo)diiron(III) complex of bpmen is reported to be catalytically inactive towards hydrocarbons [46].

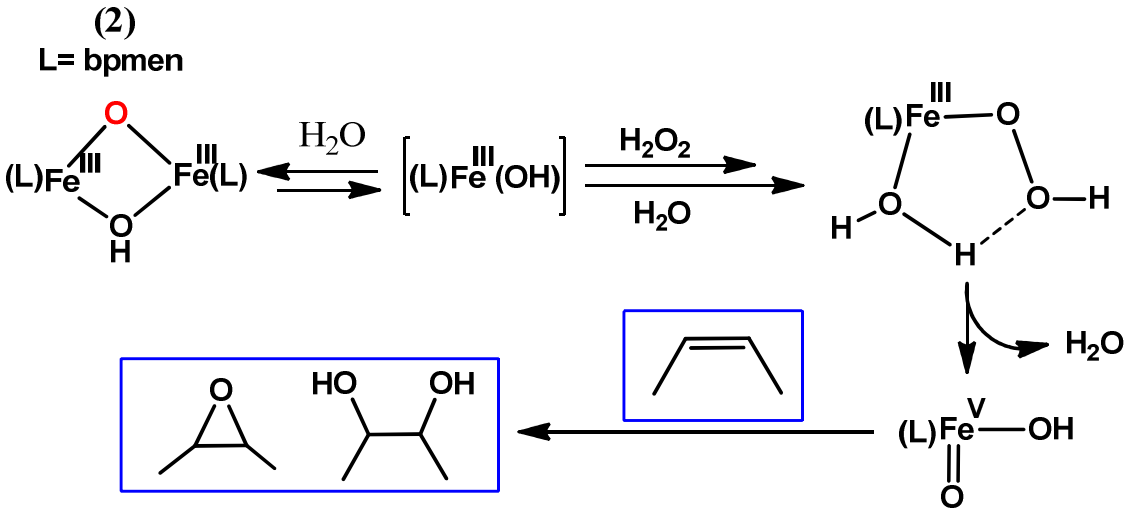

Scheme III.4 Proposed mechanism for the olefin oxidation by **2**/H_2O_2.

The mechanism of olefin oxidation by the present catalytic system is not completely clear to us. However, based on the experimental findings the sequence shown in Scheme III.4 seems reasonable. The diiron(III) complex (**2**) reacts with the oxidant(H_2O_2) to generate a high-spin mononuclear iron(III) complex, $[(bpmen)Fe^{III}(OH)]^{2+}$. This is followed by the formation of the ferric hydroperoxo species, $[Fe^{III}(OOH)(H_2O)]^{+}$ (not detected at room temperature). Heterolytic cleavage of the O-O bond of the ferric hydroperoxo generates the *cis*-HO-Fe^{V}=O oxidant capable of oxidizing olefins into epoxides and *cis*-diols. Finally, Fe^{III}-OH iron(III) species combine to form the open core Fe(III)–(μ-O)–Fe(III) complex, $[(bpmen)(H_2O)Fe(\mu\text{-}O)Fe(OH)\ (bpmen)]^{3+}$ (**2'**), which reacts with additional H_2O_2 to drive further oxidation of olefinic substrates.

III.3. Conclusion

1) In summary, the (μ-oxo diiron(III) complex $[Fe_2(\mu\text{-}O)(\mu\text{-}OH)(bpmen)_2]$ (**2**) has emerged as an useful catalyst with H_2O_2 in epoxidation of olefins under conditions of limiting substrates at room temperature.

2) Excellent substrate conversions have been obtained in presence of acetic acid.

3) The catalytic system has been shown to epoxidize electron-rich olefins, whereas *cis*-dihydroxylation is favoured in case of electron-deficient olefins. Infact, unlike the nonheme diiron(III) catalysts explored so far, the present catalytic system exhibits very high selectivity in *cis*-dihydroxylation of electron-deficient olefins under ambient reaction conditions.

4) The (μ-oxo) diiron(III) complex has been found to dissociate in solution to form monoiron species, which are believed to mitigate olefin epoxidation with hydrogen peroxide. The (μ-oxo) diiron(III) has been found to regenerate at the end of catalytic turnovers. Interestingly, the open-core oxo-bridged diiron(III) complex has been found to be catalytically potent. The regenerated complex (**2'**) shows a greater preference in *cis*-dihydroxylation of electron-deficient alkenes than the parent catalyst.

5) Furthermore, given the easy preparation and handling of the diiron(III) catalyst as well as the atom-economy of the process, the present catalytic system appears promising for the application in synthetic organic chemistry.

III.4. Experimental Section

III.4.1. General

All reagents and chemicals were purchased from sigma Aldrich and were used without further purification unless noted otherwise. 2-Picolyl chloride, N,N´-dimethylethylenediamine and $Fe(ClO_4)_3$, $10H_2O$ were purchased from Sigma Aldrich. HPLC grade Acetonitrile (HPLC, S.D. Fine Chem. Ltd., India) and ethanol (Merck, Germany) were used as received. The exact active oxygen content of H_2O_2 (30% w/v) was determined iodometrically prior to use. The UV-Vis spectra were recorded on a Agilent 8453 Spectrophotometer. Elemental Microanalysis (CHN) was done in Vario EL-III elementary analyser. The ^{1}H NMR spectrum was recorded on a Bruker spectrometer operating at 300 MHz**.** The product analyses were done by Perkin Elmer Clarus-500 GC with FID (Elite-I, Polysiloxane, 15-meter column). ESI-MS data were collected on a MICROMASS QUATTRO II triple quadrupole mass spectrometer.

III.4.2. Synthesis of the ligand and the metal complex $[(bpmen)_2Fe_2O(\mu\text{-}O)(\mu\text{-}OH)](ClO_4)_3$:

The ligand bpmen (bpmen = N,N'-dimethyl-N,N'-bis(2-pyridylmethyl)-1,2-diaminoethane) was synthesized according to the following procedure [31] and the complex (**2**) is synthesized by the known literature procedure [30]. The detailed procedure is given already in chapter II.

III.4.3. Reaction Conditions for catalytic experiments using Limiting Substrates:

III.4.3.1. Method A:

A total of 150 µL of a 0.5 mM H_2O_2 solution (diluted from a 30% H_2O_2 solution) in CH_3CN was delivered all at once in air to a CH_3CN solution (2.0 mL) containing catalyst **2** (1.25 mM, 5 mol%) catalyst and 25 mM olefin substrate. The final ratios of the catalyst, substrate and the oxidant are given in Table 1 in the main text. In various experiments, acetic acid (1 equiv *w.r.t.* the catalyst) was added to the initial solution prior to the addition of oxidant. The solution was stirred for 5 min. In all cases, the resulting solutions were treated with acetic anhydride (1.0 mL) together

with 1-methylimidazole (0.1 mL) to esterify the diol products. Iodopentafluorobenzene was added as an internal standard. Organic products were extracted with $CHCl_3$, and the solution was washed with 1M H_2SO_4, sat. $NaHCO_3$, and H_2O. The organic layer was dried with $MgSO_4$ and the solution was subjected to GC analysis. The products were identified by comparison of their GC retention times with those of aunthetic compounds. All experiments were run at least in duplicate, the reported data being the average of these reactions.

III.4.3.2. Method B:

A total of 150 µL of a 0.5 mM H_2O_2 solution (diluted from a 30% H_2O_2 solution) in CH_3CN was delivered by a syringe pump over a period of 15 mins (Rate: 0.6 mL/h) to an acetonitrile solution (2.0 mL) containing catalyst **2** (1.25 mM) and 25 mM olefin substrate. The reaction mixture was further stirred for 15 min. Identification and quantification of the products were performed according to the procedure outlined in Method A.

III.4.3.3. Method C:

A 10 mL vial was charged with the following: catalyst (2.5 µmol), substrate (250 µmol), and acetic acid (1 equiv. w.r.t catalyst) and a magnetic stir bar. The vial was placed on a stir plate and stirred vigorously at room temperature. A solution of H_2O_2 (250 µL) was added dropwise *via* syringe pump over 15 min. After stirring for 15 mins, a solution of catalyst (2.5 µmol), and acetic acid (2.5 µmol) was added via syringe. This was followed by H_2O_2 (250 µL) with the aid of syringe pump over 15 mins. After being stirred for 15 mins a third addition was performed in the same manner for a total of 7.5 µmol) of catalyst, 7.5 µmol AcOH, and 1.5 equiv H_2O_2. Each addition was allowed to stir for 15 mins, for a total reaction time of 45 min.

III.4.3.4. Method D:

Same as Method B except that additional aliquots of oxidant and substrate were delivered via syringe pump at the end of the catalytic reactions. Identification and quantification of the products were performed according to the procedure outlined in Method A.

III.4.4. Competitive olefin oxidation reactions

Three substrates were selected for pairwise competition experiments, where equimolar amounts of two different substrates were oxidized according to the procedure outlined in Method B (see above).

III.4.5. Reactions performed with the regenerated catalyst (2′)

A total of 150 µL of a 0.5 mM H_2O_2 solution (diluted from a 30% H_2O_2 solution) in CH_3CN was delivered by syringe pump over 15 min at 25ºC in air to a CH_3CN solution (2.0 mL) containing iron 1.25 mM catalyst and 1 equiv. acid with respect to catalyst. The final ratio is catalyst: acid: oxidant=1:1:30. After 15 mins of stirring, equimolar (25 mM) amounts of cyclooctene and tert-butyl acrylate was added. After the addition, 1 equiv. of acid (1.25 mM) and 150 µL of a 0.5 mM H_2O_2 solution (diluted from a 30% H_2O_2 solution) in CH_3CN was delivered by syringe pump over 15 min. The solution was further stirred for 15 min. After that, it was treated with acetic anhydride (1 mL) and 1-methylimidazole (0.1 mL) to esterify the diol products and followed work up under the normal catalytic condition explained above.

References

1. H. C. Kolb, M. S. VanNieuwenhze, K. B. Sharpless, *Chem. Rev.*, 1994, **94**, 2483.
2. S. Caron, R. W. Dugger, S. G. Ruggery, J. A. Ragan, D. H. B. Ripin, *Chem. Rev.*, 2006, **106**, 2943.
3. M. Costas, M. P. Mehn, M. P. Jensen, L. Que, Jr., *Chem. Rev.*, 2004, **104**, 939.
4. G. B. Shul'pin, *Mini-Rev. Org. Chem.*, 2009, **6**, 95.
5. G. Dubois, A. Murphy, T. D. P. Stack, *Org. Lett.*, 2003, **5**, 2469.
6. P. D. Oldenberg , L. Que, Jr., *Catal. Today*, 2006, **117**, 15.
7. P. D. Oldenberg, Y. Feng, I. Pryjomska-Ray, D. Ness, L. Que, Jr., *J. Am. Chem. Soc.*, 2010, **132**, 17713.
8. D. E. De Vos, S. de Wilderman, B. F. Sels, P. J. Grobet, P. A. Jacobs, *Angew. Chem. Int. Ed*., 1999, **38**, 980.
9. J. W. de Boer, J. Brinksma, W. R. Browne, A. Meetsma, P. L. Alsters, R. Hage, B. L. Ferringa, *J. Am. Chem. Soc.*, 2005, **127**, 7990.
10. P. C. A. Bruijnincx, I. L. C. Buurmans, S. Gosiewska, M. A. H. Moelands, M. Lutz, A. L. Spek, G.Van Koten, R. Gebbink, *Chem. Eur. J.*, 2008, **14**, 1228.
11. S. Chatterjee, T.K. Paine, *Angew. Chem. Int. Ed.*, 2015, **54**, 9338
12. T. W. S. Chow, E. L. M. Wong, Z. Guo, Y. Liu, J. S. Huang, C. M. Che, *J. Am. Chem. Soc.*, 2010, **132**, 13229.
13. M. Costas, *Coord. Chem. Rev*., 2011, **255**, 2912.
14. E. A. Mikhalyova, O. V. Makhlynets, T. D. Palluccio, A. S. Filatov, E. V. Rybak-Akimova, *Chem. Commun.*, 2012, **48**, 687.
15. S. Taktak, W. H. Ye, A. M. Herrera, E. V. Rybak-Akimova, *Inorg. Chem.*, 2007, **46**, 2929.
16. (a) A. L. Feig, S. J. Lippard, *Chem. Rev.*, 1994, **94**, 759; (b) B. J. Wallar, J. D. Lipscomb, *Chem. Rev*., 1996, **96**, 2625.
17. S. R. Iyer, M. M. Javadi, Y. Feng, M.Y. Hyun, W. N. Oloo, C. Kim,L. Que, Jr., *Chem. Commun*., 2014, **50**, 13777 and the references therein.
18. M. Fujita, M. Costas, L. Que, Jr., *J. Am. Chem. Soc.*, 2003, **125**, 9912.
19. R. Mas-Balleste, L. Que, Jr., *J. Am. Chem. Soc.*, 2007, **129**, 15964.
20. W. N. Oloo, A. J. Fielding, L. Que, Jr., *J. Am. Chem. Soc.*, 2013, **135**, 6438.
21. I. Prat, J. S. Mathieson, M. Guell, X. Ribas, J. M. Luis, L. Cronin, M. Costas, *Nat. Chem.*, 2011, **3**, 788.
22. E. Y. Tshuva, S. J. Lippard, *Chem. Rev.*, 2004, **104**, 987.
23. J. R. Hartman, R. L. Rardin, P. Chaudhury, K. Pohl, K. Wieghardt, B. Nuber, J. Weiss, G. C. Papaefthymiou, R. B. Frankel, S. J. Lippard, *J. Am. Chem. Soc.*, 1987, **109**, 7387.
24. E. Y. Tshuva, D. Lee, W. Bu, S. J. Lippard, *J. Am. Chem. Soc.*, 2002, **124**, 2416.
25. K. Chen, M. Costas, L. Que, Jr., J. Chem. Soc. *Dalton Trans.*, 2002, 672.
26. K. Chen, M. Costas, J. H. Kim, A. K. Tipton, L. Que, Jr., *J. Am. Chem. Soc.*, 2002, **124**, 3026.

27. (a) M. Kodera, M. Itoh, K. Kano, T. Funabiki, M. Reglier, *Angew. Chem. Int. Ed.*, 2005, **44,** 7104; (b) M. Kodera, Y. Kawahara, Y. Hitomi, T. Nomura, T. Ogura, Y. Kobayashi, *J. Am. Chem. Soc.*, 2012, **134**, 13236.
28. M. C. White, A. G. Doyle, E. N. Jacobsen, *J. Am. Chem. Soc.*, 2001, **123**, 7194.
29. (a) E. A. Duban, K. P. Brylyakov, E. P. Talsi, *Eur. J. Inorg. Chem.*, 2007, 852; (b) E. A. Duban, K. P. Brylyakov, E. P. Talsi, *Kinet. Catal.*, 2008, **49**, 379.
30. (a) A. Hazell, K. B. Jensen, C. J. McKenzie and H. Toftlund, *Inorg. Chem.*, 1994, **33**, 3127; (b) S. Taktak, S.V. Kryatov, E.V. Rybak-Akimova, *Inorg. Chem.*, 2004, **43**, 7196.
31. A. Iturrospe, B. Artetxe, S. Reinoso, L. S. Felices, P. Vitoria, L. Lezama, J. M. Gutiérrez-Zorrilla, *Inorg. Chem.*, 2013, **52**, 3084.
32. R. E. Norman, R. C. Holz, S. Menagel, C. J. O'Connor, J. H. Zhang, L. Que, Jr., *Inorgchem.*, 1990, **29**, 4629.
33. R. C. Reem, J. M. McCormick, D. E. Richardson, F. J. Devlin, P. J. Stephens, R. L. Musselman, E. I. Solomon, *J. Am. Chem. Soc.*, 1989, **111**, 4688.
34. R. C. Holz, T. E. Elgren, L. L. Pearce, J. H. Zhang, C. J. O'Connor, L.Que, Jr., *Inorg. Chem.*, 1993, **32**, 5844.
35. Y. Zang, G. Pan, L. Que, Jr., B. G. Fox, E. Münck, *J. Am. Chem.Soc.*, 1994, **116**, 3653.
36. P. Saisaha, D. Pijper, R. P. van Summeren, R. Hoen, C. Smit, J.W. de Boer, R. Hage, P. L. Alsters, B. L. Ferringa, W. R. Browne, *Org. Biomol. Chem.*, 2010, **8**, 4444.
37. M. Fujita and L. Que, Jr., *Adv. Synth. Catal.*, 2004, **346**, 190.
38. Q. Zhang and C. R. Goldsmith, *Inorg. Chem.* 2014, **53**, 5206.
39. The yields are based on the initial substrate concentrations. Thus, 44.0 µmol oxygenates from the oxidation of *cis*-cyclooctene and 22.0 µmol oxygenates from *tert*-butyl acrylate oxidation are obtained. The products account for ~88% of the oxidant added to the regenerated catalyst.
40. I. Prat, A. Company, V. Postils, X. Ribas, L. Que, Jr., J. M. Luis, M. Costas, *Chem. Eur. J.*, 2013, **19**, 6724.
41. Y. Feng, J. England, L. Que, Jr., *ACS Catal.*, 2011, **1**, 1035.
42. I. Prat, J. S. Mathieson, M. Guell, X. Ribas, J. M. Luis, L. Cronin, M. Costas, *Nat. Chem.*, 2011, **3**, 788.
43. (a) T. D. H. Bugg, S. Ramaswamy, *Curr. Opin. Chem. Biol.*, 2008, **12**, 134; (b) S. M. Barry, G. L. Challis, *ACS Catal.*, 2013, **3**, 2362.
44. O.Y. Lyakin, A. M. Zima, D. G. Samsonenko, K. P. Bryliakov, E. P. Talsi, *ACS Catal.*, 2015, **5**, 2702.
45. S. Poussereau, G. Blodin, M. Cesario, J. Guilhem, G. Chottard, F. Gonnet, J.-J. Girerd, *Inorg. Chem.*, 1998, **37**, 3127.
46. J. Y. Ryu, J. Kim, M. Costas, K. Chen, W. Nam, L. Que., Jr. *Chem. Commun.*, 2002, 1288.